Les Cahiers du GERAD ISSN: 0711–2440

Joint fleet management and stochastic short-term production planning in mining complexes with carbon footprint reduction

V. Balboa-Espinoza, R. Dimitrakopoulos

G–2025–71

October 2025

La publication de ces rapports de recherche est rendue possible grâce au soutien de HEC Montréal, Polytechnique Montréal, Université McGill, Université du Québec à Montréal, ainsi que du Fonds de recherche du Québec – Nature et technologies.

Dépôt légal – Bibliothèque et Archives nationales du Québec, 2025
– Bibliothèque et Archives Canada, 2025

The publication of these research reports is made possible thanks to the support of HEC Montréal, Polytechnique Montréal, McGill University, Université du Québec à Montréal, as well as the Fonds de recherche du Québec – Nature et technologies.

Legal deposit – Bibliothèque et Archives nationales du Québec, 2025
– Library and Archives Canada, 2025

GERAD HEC Montréal
3000, chemin de la Côte-Sainte-Catherine
Montréal (Québec) Canada H3T 2A7

Tél. : 514 340-6053
Téléc. : 514 340-5665
info@gerad.ca
www.gerad.ca

Joint fleet management and stochastic short-term production planning in mining complexes with carbon footprint reduction

Victor Balboa-Espinoza [a, b]

Roussos Dimitrakopoulos [a, b]

[a] *COSMO – Stochastic Mine Planning Laboratory Department of Mining and Materials Engineering, McGill University, Montréal (Qc), Canada, H3A 0E8*

[b] *GERAD, Montréal (Qc), Canada, H3T 1J4*

victor.balboa-espinoza@mail.mcgill.ca
roussos.dimitrakopoulos@mcgill.ca

October 2025
Les Cahiers du GERAD
G–2025–71

Abstract : Mining complexes face increasing pressure to reduce environmental impacts, yet most short-term stochastic optimization frameworks in mining complexes neglect environmental objectives, focusing solely on economic and operational performance. This work extends the framework by incorporating carbon footprint and pricing schemes under uncertainty, explicitly accounting for variability in emission factors and truck trip distributions. A parallelized reactive GRASP metaheuristic solution approach is adapted and used for its scalability, flexibility, and effectiveness in navigating large, non-linear search spaces. Experimental results for a gold mining complex demonstrate up to 4% emission reductions from truck and shovels operation with only a 0.4% loss in profit.

Keywords : Short-term stochastic production planning; fleet management; stochastic mathematical programming; sustainable stochastic optimization; carbon footprint reduction; metaheuristic optimization

---

Acknowledgements: The work in this paper was funded by the National Sciences and Engineering Research Council (NSERC) of Canda CRD Grant 500414-16, the NSERC Discovery Grant 239019, and the industry consortium members of COSMO Stochastic Mine Planning Laboratory (AngloGold Ashanti, Anglo American/DeBeers, Agnico Eagle, BHP, IAMGOLD, Kinross Gold, Newmont, and Vale), and the Canada Research Chairs Program.

1 Introduction

The mining industry plays a key role in supplying materials for infrastructure, energy, electronics, and manufacturing (Carvalho, 2017; Amegboleza and Ülkü, 2025). As global demand for minerals continues to grow due to their role in key energy technologies for decarbonization (Calderon et al., 2020; De Donno, 2024; Kamran et al., 2023), the sector faces increasing pressure to optimize operations that balance economic results and environmental impacts (Laurence, 2011; Moran et al., 2014; Suorineni, 2022). At the same time, recent climate impacts, primarily generated by the worldwide carbon emissions (Liu et al., 2021; Matthews et al., 2008), have intensified calls for reductions in Greenhouse Gas (GHG) emissions to mitigate the long-term risks associated with global warming and climate instability (Nema et al., 2012; Mora et al., 2018). Mining companies, which are responsible for an estimated 8-10% of global carbon emissions (Yokoi et al., 2022; Huo et al., 2023; Rachid et al., 2023), therefore face new social, regulatory, and environmental responsibilities, making the integration of environmental performance into mine production planning a critical and urgent challenge.

In open-pit operations, nearly 30% of the total energy consumption is attributed to truck and shovel equipment operation (Nikbin et al., 2025), 36-50% arises from the comminution in the processing stage (Ballantyne and Powell, 2014; Jeswiet and Szekeres, 2016), while the remaining is consumed at non-comminution and other stages (e.g. drilling and blasting, auxiliary services). Because the loading and hauling stage relies primarily on diesel combustion (unlike the comminution stage, where the primary source is electricity), truck and shovel operations arise as a key emission source, contributing almost 50% of the total GHG emissions from mining activities (Norgate and Haque, 2010; Nikbin et al., 2025). Nevertheless, despite its operational and environmental importance, equipment operation is often optimized independently from mine production planning, resulting in operation inefficiencies and higher GHG emissions.

Several works have attempted to integrate material extraction scheduling and fleet management to capture synergies typically lost when these steps are optimized independently (Fioroni et al., 2008; L'Heureux et al., 2013; Torkamani and Askari-Nasab, 2015; Mousavi et al., 2016; Blom et al., 2017; Kozan and Liu, 2018). However, most of these models overlook geological uncertainty as a main precursor of past project failures (Vallée, 2000), as well as other sources of uncertainty, such as the equipment and processing plant performance uncertainties. Addressing this limitation and recognizing the impact of not modelling these uncertainties, Villalba Matamoros and Dimitrakopoulos (2016) jointly optimized short-term scheduling and fleet allocation decisions for a single mine under geological and equipment uncertainty via a cost-based stochastic integer programming (SIP) model. Building on that, Quigley and Dimitrakopoulos (2020) extended the formulation to optimize multiple mines and processing streams simultaneously, known as mining complex optimization, while also adding horizontal constraints to account for hauling ramp locations. Subsequently, Both and Dimitrakopoulos (2020) embedded the previous works into the stochastic global optimization framework for open pit mining complexes (Goodfellow and Dimitrakopoulos, 2016). The approach enabled the joint optimization of multiple linear and non-linear aspects of the mining complexes within a single formulation. At the same time, it also incorporated major components of short-term mine production planning, such as the scheduling of a heterogeneous truck fleet and individual shovel allocations, while also accounting for geological and equipment uncertainty, along with operational costs and production losses.

Although existing models represent important progress in jointly optimizing scheduling and fleet decisions under uncertainty, they remain centered on operational and economic performance, omitting environmental considerations, which are becoming critical drivers of decision-making. To address this gap, several studies have incorporated environmental impacts into the mine production planning optimization (Pell et al., 2019; Xu et al., 2018; Xu et al., 2021; Amirmoeini et al., 2024; Mirzehi and Moradi Afrapoli, 2024a, 2024b, 2024c). However, all these studies either incorporate environmental aspects only within long-term production scheduling, overlooking that most decarbonization strategies are implemented at the short-term level, or neglect the role of uncertainty, both in production forecasts and equipment performance, which critically influences emissions outcomes.

Pell et al. (2019) combined the life cycle assessment methodology and the long-term mine scheduling optimization process to limit global warming impacts from mineral extraction. This approach led to an 8.1% reduction in the global warming indicator, but at a cost of a 4.1% reduction of the Net Present Value (NPV) of the project. Xu et al. (2018) found that, for their specific case study, by incorporating different ecological costs, the extraction schedule changes considerably, reducing the NPV by 7.47 MUS$. In another study, Xu et al. (2021) introduced environmental and social indicators to optimize the open-pit limit on a metal mine in northeastern China. The optimization resulted in a 37.5% smaller pit when ecological costs are incorporated and a 48.3% larger pit when social benefits (e.g., medical care expenditures, training and reeducation investments) are considered. Similarly, Amirmoeini et al. (2024) incorporated carbon costing in the mathematical optimization model. Scenarios with and without carbon emission constraints were compared across three different orebody models, finding that when no carbon emission constraints are introduced, a higher NPV is obtained in all cases. Mirzehi and Moradi Afrapoli (2024a, 2024b, 2024c) presented three related studies that addressed similar operational goals in long-term mine planning optimization but approached the problem using different mathematical formulations. Although the modelling strategies varied, their findings converged on a common insight: incorporating environmental constraints or carbon costing strategies into the optimization can lead to a reduction in carbon emissions, although at the expense of a lower NPV.

To address the absence of joint fleet management and stochastic short-term production planning frameworks with carbon footprint considerations under uncertainty, the present work builds upon the contributions of Both and Dimitrakopoulos (2020). It does so by incorporating carbon footprint as an explicit environmental optimization component that quantifies the carbon dioxide emissions (Wiedmann and Minx, 2008), enabling the assessment of carbon pricing and accounting for the strategies' impacts on short-term material scheduling and fleet operations under geological and equipment performance uncertainty. Additionally, two new sources of uncertainty are introduced: 1) variability in emission factors due to truck and shovel combustion efficiencies, and 2) variability in the trip distributions across heterogeneous truck fleets. Finally, the proposed model is solved using a reactive Greedy Randomized Adaptive Search Procedure (rGRASP) with cooperative parallelization (Ribeiro and Rosseti, 2007); this approach is chosen due to its efficiency in solving large-scale combinatorial problems, its simple implementation, and its parallelization capabilities to exploit modern computational resources (Festa and Resende, 2002).

In the following sections, the mathematical stochastic model of mining complexes that account for a carbon footprint is presented, followed by the metaheuristic solving approach. Next, a case study is performed at a gold mining complex where different carbon pricing system scenarios are compared. Finally, conclusions are presented.

2 Method

2.1 Mathematical formulation

The mathematical model is formulated as a stochastic integer programming model with fixed recourse (Birge and Louveaux, 2011), based on the formulation proposed by Both and Dimitrakopoulos (2020), referred here as the "original problem." The stochastic integer programming formulation is described next.

2.1.1 Notation and definitions

This section introduces the notation and definitions used in the mathematical formulation. All the indices and sets are presented in Table 1. The parameters and decision variables are observed in Table 2 and Table 3, respectively.

Table 1: Indices and sets used in the mathematical formulation.

Indices/sets	Description
$t \epsilon \mathbb{T}$	Index of a discretized time period over a defined planning horizon $\|\mathbb{T}\|$
$s \epsilon \mathbb{S}$	Index of an orebody scenario in the set of orebody scenarios $\mathbb{S}$
$s_e \epsilon \mathbb{S}_e$	Index of an equipment performance scenario in the set of equipment scenarios $\mathbb{S}_e$
$s_o \epsilon \mathbb{S}_o$	Index of a truck-fleet operation performance scenario in the set of truck fleet operation performance scenarios $\mathbb{S}_o$
$s_c \epsilon \mathbb{S}_c$	Index of a carbon footprint factor scenario in the set of carbon footprint factor scenarios $\mathbb{S}_c$
$\varepsilon \epsilon \mathbb{P} \cup \mathbb{H}$	Index of an attribute from the set of primary attributes $\mathbb{P}$ and hereditary ones $\mathbb{H}$
$d \epsilon \mathbb{D}$	Index of a destination in the set of destinations $\mathbb{D}$
$a \epsilon \mathbb{A}$	Index of a mining area in the set of all mining areas $\mathbb{A}$
$i \epsilon \mathbb{A} \cup \mathbb{D}$	Index of a location i in the mining complex, in the set of all the possible locations
$b \epsilon \mathbb{B}$	Index of a mining block in the set of all blocks $\mathbb{B}$
$c \epsilon \mathbb{C}$	Index of a cluster c of material in the set of all clusters $\mathbb{C}$
$i \epsilon \mathbb{L}$	Index of a shovel operating across the mining complex in the set of all shovels $\mathbb{L}$
$m \epsilon \mathbb{M}$	Index of a truck-type operating across the mining complex in the set of all truck-types $\mathbb{M}$

Table 2: Parameters used in the mathematical formulation.

Parameter	Description
$p_{h,i,t}$	Unit price of the hereditary attribute h at location i in period t
$c^+_{\varepsilon,t}$, $c^-_{\varepsilon,t}$	Cost penalties for excess or shortage of a primary attribute ε, respectively
Ton_b	Tonnage of a block b
H^t	Scheduled working hours in period t
$CostSmooth$	Penalty cost for not extracting all adjacent block of block b in the same period where b is extracted
L^{Max}_a	Maximum number of shovels that can work simultaneously in the same area a
T^{Max}_m, T^{Min}_m	Maximum and minimum number of trucks of truck-type m that can be scheduled
$Prod^t_{l,s_e}$	Stochastic production rate for shovel l in period t under equipment scenario s_e
Cap_m	Nominal capacity of truck-type m
A^t_{m,s_e}	Stochastic availability of truck-type m in period t under equipment scenario s_e
$CT_{b,s}$	Truck cycle time required to transport material from a block b to its destination defined under scenario s
$CostOpTruck_m$	Operational cost of having a truck-type m working
$CostMove_{l,a,a'}$	Moving cost for shovel l between areas a (from) and $a^{'}$ (to)
$LostProd_{l,a,a'}$	Production lost for transporting a shovel l between areas a (from) and $a^{'}$ (to)
$CostShovelShortage$	Penalty cost for each tonne not extracted due to inefficient shovel allocation
$CostTruckShortage$	Penalty cost for each tonne not extracted due to inefficient truck fleet dimensioning
CCF^+_t	Penalty cost for each unit of carbon footprint over the carbon footprint limit in period t
BCF^-_t	Benefits obtained for being under the carbon footprint limits in period t
α_{b,m,s_o}	Relative (proportion) material transported from block b by truck-type m under the operational performance scenario s_o
CF_{s_c}	Carbon footprint factor under scenario s_c
CF^{limit}_t	Carbon footprint limit in period t
$FC_{l,a,a'}$	Fuel consumed by shovel l when is transported from area a to area $a^{'}$
$\widehat{FCtruck}_{b,s,m}$	Fuel consumed by truck-type m to transport all the material from source block location b to destination defined under scenario s

2.1.2 Objective function

The original problem seeks to maximize profit under short-term planning considerations, while managing production targets, simultaneously capturing the interrelations among the different decisions, and the synergies that arise when extraction sequencing and equipment allocation are jointly optimized. The proposed formulation extends the objective function by incorporating an additional component (Part VIII) that accounts for carbon footprint deviations and associated pricing.

Table 3: Decision variables used in the mathematical formulation.

Variable	Description
x_b^t	Binary variable representing if block b is extracted at period t ($x_b^t = 1$) or not (t$x_b^t = 0$)
$z_{c,d}^t$	Binary variable representing if cluster c is sent to destination d at period t ($z_{c,d}^t = 1$) or not ($z_{c,d}^t = 0$)
$\lambda_{l,a}^t$	Binary variables representing if shovel l is located in area a at period t ($\lambda_{l,a}^t = 1$) or not ($\lambda_{l,a}^t = 0$)
$\omega_{l,a,a'}^t$	Binary variable representing if shovel l has moved from area a to area $a^{'}$ at period t ($\omega_{l,a,a'}^t = 1$) or not ($\omega_{l,a,a'}^t = 0$)
τ_m^t	Integer variables which represent the number of trucks of truck-type m required in period t
$\delta_{d,r,s}^t$	Continuous variable, between 0 and 1, that represents the proportion of material sent from destination d to destination r under scenario s at period t
$dshovel_{a,s_e}^t$	Continuous variables representing shovel production deviations in area a under equipment scenario s_e at period t
$dtruck_{s,s_e,m}^t$	Continuous variable representing haulage capacity deviations for each location defined by scenario s under equipment scenario s_e at period t for truck type m
dcf_{t,s_c}^+ , dcf_{t,s_c}^-	Continuous variables representing carbon footprint deviations from carbon footprint limits, both excess and shortage, respectively
$d_{\varepsilon,i,t,s}^+$, $d_{\varepsilon,i,t,s}^-$	Continuous variables modelling either surplus or shortage of attribute ε at location i in period t under scenario s
$v_{p,i,t,s}$	Continuous variable which represents the value of primary attribute p at location i in period t, under scenario s
$v_{h,i,t,s}$	Continuous variable which represents the value of hereditary attribute h at location i in period t, under scenario s

$$
\begin{aligned}
\max \quad & \underbrace{\frac{1}{\|\mathbb{S}\|}\sum_{t\in\mathbb{T}}\sum_{s\in\mathbb{S}}\sum_{h\in\mathbb{H}}\sum_{i\in\mathbb{A}\cup\mathbb{D}} p_{h,i,t}v_{h,i,t,s}}_{\text{Part I. Revenues and costs of mining complex}} \\
& \underbrace{-\frac{1}{\|\mathbb{S}\|}\sum_{t\in\mathbb{T}}\sum_{s\in\mathbb{S}}\sum_{i\in\mathbb{A}\cup\mathbb{D}}\sum_{\varepsilon\epsilon\mathbb{P}\cup\mathbb{H}} c_{\varepsilon,t}^+ d_{\varepsilon,i,t,s}^+ + c_{\varepsilon,t}^- d_{\varepsilon,i,t,s}^-}_{\text{Part II. Deviations from production targets}} \\
& \underbrace{-\frac{1}{\|\mathbb{S}_e\|}\sum_{t\in\mathbb{T}}\sum_{s_e\in\mathbb{S}_e}\sum_{a\in\mathbb{A}} CostShovelShortage\cdot dshovel_{a,s_e}^t}_{\text{Part III. Cost of not achieving shovel production target}} \\
& \underbrace{-\sum_{t\in\mathbb{T}\setminus\{1\}}\sum_{l\in\mathbb{L}}\sum_{a\in\mathbb{A}}\sum_{a'\in\mathbb{A}\{a\}} CostMove_{l,a,a'}\omega_{l,a,a'}^t}_{\text{Part IV. Cost of shovel movement}} \\
& \underbrace{-\frac{1}{\|\mathbb{S}\cdot\mathbb{S}_e\cdot\mathbb{S}_o\|}\sum_{t\ \in\mathbb{T}}\sum_{s_e\in\mathbb{S}_e}\sum_{s\in\mathbb{S}}\sum_{s_o\in\mathbb{S}_o}\sum_{m\in\mathbb{M}} CostTruckShortage\cdot dtruck_{s,s_e,s_o,m}^t}_{\text{Part V. Truck fleet haulage capacity}} \\
& \underbrace{-\sum_{t\in\mathbb{T}}\sum_{m\in\mathbb{M}} CostOpTruck\cdot\tau_m^t}_{\text{Part VI. Cost of truck operation}} \ \underbrace{-\sum_{t\in\mathbb{T}}\sum_{b\in\mathbb{B}} CostSmooth\cdot y_b^t}_{\text{Part VII. Smooth mining schedule}} \\
& \underbrace{-\frac{1}{\|\mathbb{S}_c\|}\sum_{t\in\mathbb{T}}\sum_{s_c\in\mathbb{S}_c} CCF_t^+\cdot dcf_{t,s_c}^+ - BCF_t^-\cdot dcf_{t,s_c}^-}_{\text{Part VIII. Costs/benefits of deviating from carbon footprint limits}}
\end{aligned}
\tag{1}
$$

Part I of the objective function encompasses the revenues from the products generated at each location, as well as the operational cost required to produce the materials. Part II accounts for the deviations from production targets that occur at each location for each attribute, as presented by

Goodfellow and Dimitrakopoulos (2016, 2017). Part III accounts for the penalties of deviating from the required shovel production at each area and period. Part IV summarizes the costs linked to the shovel movement. Part V accounts for the penalties of deviating from truck haulage requirements for each period. Part VI sums up the cost of having a certain number of truck types m operating across the mining complex. Part VII enforces the extraction of adjacent mining blocks at the same period to generate connected patterns, as presented by Dimitrakopoulos and Ramazan (2004). The last term (part VIII) is introduced in this new extension to capture both the penalties of having an excess of carbon footprint and the benefits or rewards of falling below the carbon footprint limits. This term acts as a tool to evaluate different carbon pricing scenarios and permits to study the impact of new norms around carbon footprint, and its impact on fleet management and material extraction sequencing.

2.1.3 Constraints

All constraints related to the reserve, precedence, ore targets, deleterious elements, as well as downstream flows considering stockpiles and other locations are presented and used as in Goodfellow and Dimitrakopoulos (2016). Constraints related to fleet management are mostly used as presented in the original problem by Both and Dimitrakopoulos (2020), with the exceptions presented here.

The variability of trip distribution is introduced in the formulation through the parameter α_{b,m,s_o} (Table 2). This parameter represents the truck operational performance by measuring the ratio between the material transported by a truck-type m from a source block b and the total material mass supplied by the block b in scenario s_o. Since operational performance is influenced by factors such as queuing times, speed variability, and delays at intersections or crossings, all elements that are difficult to estimate deterministically and that ultimately affect the production of each truck type, α_{b,m,s_o} are modeled stochastically and discretized into the $s_o \in \mathbb{S}_o$ scenarios. For each block and truck type, values can be generated from empirical distributions obtained from real operational data or simulated using Discrete Event Simulation (DES) techniques.

Accordingly, the truck fleet haulage constraint proposed by Both and Dimitrakopoulos (2020) is modified to incorporate the variability of trips for each truck-type, which defines their operational performance, while simultaneously dimensioning the truck fleet under uncertain performance (Equation (2)).

$$Cap_m \cdot A^t_{m,s_e} \cdot H^t \cdot \tau^t_m \; - \sum_{b \epsilon \mathbb{B}} CT_{b,s} \cdot Ton_b \cdot x^t_b \cdot \alpha_{b,m,s_o} + dtruck^t_{s,s_e,s_o,m} \geq 0$$
$$\forall t \in \mathbb{T}, s_e \in \mathbb{S}_e, s \in \mathbb{S}, m \in \mathbb{M}, s_o \in \mathbb{S}_o \quad (2)$$

The first term of Equation (2) reflects the actual haulage capacity of the truck fleet of type m given a stochastic simulated availability, while the second term reflects the required material extraction for that truck-type fleet under a specific expected operation performance. It is worth noting that this equation relates indirectly to the actual utilization of truck fleet type m, since the difference between the required haulage production and the maximum possible haulage production of the truck fleet (represented by the product of A^t_{m,s_e} and H^t) reflects the loss stemming from an imperfect utilization of the equipment. In this regard, the decision variable $dtruck^t_{s,s_e,s_o,m}$ inherits this factor, meaning that when its value is negative, there is a utilization less than 100% (more capacity than what is required). In this sense, the model inherently addressed truck utilization, while also determining the appropriate fleet size for each truck-type, avoiding production losses caused by an undersized fleet and preventing suboptimal truck performances from an oversized fleet.

In the case of not measuring carbon emissions, the amount of gas $e \in \mathbb{E}$ emitted can be estimated using Equation (3), adapted from the 2006 Intergovernmental Panel on Climate Change (IPCC) Guidelines for mobile combustion (IPCC, 2006). The emission factor $Ef^e_{s_c}$, is modeled stochastically since it is subject to uncertainty in the actual emissions during the equipment operation. This uncertainty

arises from multiple sources, including variability in combustion efficiency, differences in equipment age and maintenance, and fluctuations in operating conditions, such as load or empty cycle. Rather than assuming a fixed deterministic value, this stochasticity is discretized into scenarios $s_c \epsilon \mathbb{S}_c$, which represent possible realizations of the carbon footprint indicator. This approach allows the formulation to assess how different emission factors, and their associated uncertainty, affect both the material extraction schedule and equipment operation.

$$Emission_{e,\ s_c,t} = \sum_{e \in E} Ef^{e}_{s_c} \cdot EC_t \tag{3}$$

As shown by Equation (3), the energy consumed EC_t will be subject to the material extraction sequence in the period t that characterizes the final fuel consumption. In this regard, the energy consumed will be estimated differently between trucks and shovels. This approach allows the formulation to rely on energy quantification (i.e., an energy-based model) and enables the incorporation of future decarbonization strategies, like fleet electrification (which has been identified as the most efficient decarbonization strategy (Miranda and Pourrahimian, 2024), simply by modifying the corresponding emission factors. Moreover, this model approach allows us to indirectly optimize energy consumption, regardless of its source (e.g., diesel, solar electricity), which expands the proposed framework's applicability.

Equations (4) to (6) are used to estimate the shovels, trucks, and the total emissions, respectively. The main difference between the equipment lies in the fact that truck emissions depend on the operation performance scenario s_o, which indirectly relates the number of trips done between a source location b and a destination defined by the scenario s (8).

$$ShovelEmissions_{e,s_c,t} = \sum_{e \in E} Ef^{e}_{s_c} \cdot ShovelEC_t \tag{4}$$

$$TruckEmission_{e,s_c,t} = \frac{1}{\|\mathbb{S}\|} \sum_{s \in \mathbb{S}} \sum_{e \in E} Ef^{e}_{s_c} \cdot TruckEC_{t,s} \tag{5}$$

$$TotalEmission_{e,s_c,t} = ShovelEmissions_{e,s_c,t} + TruckEmission_{e,s_c,t} \tag{6}$$

$$ShovelEC_t = \sum_{l \in \mathbb{L}} \sum_{a \in \mathbb{A}} \sum_{a' \in \mathbb{A}\{a\}} FC_{l,a,a'} \cdot \rho \cdot \delta \cdot \omega^{t}_{l,a,a'} \tag{7}$$

$$TruckEC_{t,s} = \frac{1}{|\mathbb{S}_o|} \sum_{s_o \in \mathbb{S}_o} \sum_{b \epsilon \mathbb{B}} \sum_{m \in \mathbb{M}} \widetilde{FCtruck}_{b,s,m} \cdot \alpha_{b,m,s_o} \cdot \rho \cdot \delta \cdot x^{t}_{b} \tag{8}$$

The energy consumed by each equipment type is estimated and incorporated in the mathematical model using the relations presented in Equations (7) and (8). Equation (7) reflects how each shovel movement triggered from area a to area a' in period t, will increase the actual energy consumption for that period. Similarly, as soon as the extraction of a certain block b is scheduled in period t, the energy consumed is increased by the required amount to transport the material between the locations defined (Equation (8)). Parameter $FC_{l,a,a'}$ represent the fuel consumed by a shovel l to be transported from area a to area a', while parameter $\widetilde{FCtruck}_{b,s,m}$ represents the fuel consumed by each cycle done by a truck-type m between its source block location b and the destination defined under the scenario s. It is worth noting that this factor assumes the whole material from the block b is extracted by a truck-type m , which is later adjusted by a factor α_{b,m,s_o}. Parameters ρ and δ are the fuel density and fuel Higher Heat Value (HHV), respectively. These are then used to transform fuel consumption to energy consumption. In the case of electricity-based powertrains, Equations (7) and (8) can be modified by removing the fuel-related parameters (FC, ρ, and δ) and directly linking the decision variables to electricity consumption factors.

The carbon footprint indicator, as used in the present work, is estimated using different emission factors, $Ef^{e}_{s_c}$, and a characterization factor, f^{e}, for each emission e representing the actual contri-

bution of the emission to the worldwide carbon footprint (Equation (9)). In this sense, the total carbon footprint can be calculated directly as presented by Equation (10), where the emission factor from Equations (4) and (5) is replaced by the carbon footprint indicator and incorporated inside Equation (6).

$$CF_{s_c} = \sum_{e \in E} Ef^e_{s_c} \cdot f^e \tag{9}$$

$$CarbonFootprint_{s_c,t} = CF_{s_c} \cdot (ShovelEC_t + TruckEC_t) \tag{10}$$

Given the details presented above, the carbon footprint is included in the optimization model by accounting for the deviations (dcf^+_{t,s_c}, dcf^-_{t,s_c}) between the total carbon footprint contribution from truck and shovel operations, which absorbs the variability related to truck trip distribution through the variable $TruckEC_t$, and the carbon footprint limit CF^{limit}_t for each period t and each carbon footprint scenario s_c.

$$CF^{limit}_t - CarbonFootprint_{s_c,t} + dcf^+_{t,s_c} \geq 0 \qquad \forall\ s_c \in \mathbb{S}_c, t \in \mathbb{T} \tag{11}$$

$$CarbonFootprint_{s_c,t} - CF^{limit}_t + dcf^-_{t,s_c} \geq 0 \qquad \forall\ s_c \in \mathbb{S}_c, t \in \mathbb{T} \tag{12}$$

$$dcf^+_{t,s_c}, dcf^-_{t,s_c} \geq 0 \qquad \forall\ s_c \in \mathbb{S}_c, t \in \mathbb{T} \tag{13}$$

2.2 Metaheuristic solution approach

Previous studies have shown that, although the number of blocks scheduled in the short-term is relatively small compared to long-term schedules, the number of operational decisions that must be incorporated at this scale significantly increases the problem complexity (Both and Dimitrakopoulos, 2020). Metaheuristic approaches have been shown to outperform exact optimization methods in terms of computational efficiency, while still producing solutions sufficiently close to the optimal (Lamghari et al., 2014; Montiel and Dimitrakopoulos, 2015, 2017; Goodfellow and Dimitrakopoulos, 2016, 2017; Lamghari and Dimitrakopoulos, 2012, 2020, 2022). As additional sources of uncertainty are integrated into the models (reaching nearly 7,000 scenarios in the case study presented below), the computational burden per iteration grows substantially. Therefore, improving the efficiency of the overall optimization algorithm offers considerably benefits.

The present work employs a Greedy Randomized Adaptive Search Procedure (GRASP) chosen for its efficiency in solving large-scale combinatorial problems and its simplicity for implementation and parallelization (Festa and Resende, 2002). GRASP is a multistart metaheuristic that combines a semi-greedy construction phase with a local search algorithm (Resende and Ribeiro, 2016). In each iteration, the semi-greedy phase builds an initial solution by selecting elements (inverted frustum cones centered in a reference block) randomly from a candidate list of high-ranked elements, introducing controlled randomness compared to a purely greedy approach. Once the initial solution is generated, a hyper-heuristics algorithm is used to guide this search process. The hyper-heuristic approach is adopted in the place of a traditional local search, as it can handle the multiple neighborhood structures associated with the different decision variables of the model. This search algorithm follows a greedy strategy. Figure 1 schematises how the hyper-heuristic applies all low-level heuristics, h_i, to the current solution and sets the one with the highest objective value as the new current solution for further improvement. This strategy ensures that the search will continue until no further improvements can be produced by any of the available low-level heuristics, thereby reaching a heuristic-dependent local optimum.

A key advantage of GRASP lies in its multistart nature, which relies on generating multiple initial solutions to exponentially increase the likelihood of reaching high-quality or near-optimal solutions (Aiex et al., 2002). This characteristic can be valuable for problems where the optimization outcome is highly sensitive to the starting point, as in the case of stochastic optimization of mining complexes, where different construction methods can significantly affect the final objective value (Lamghari et al., 2014).

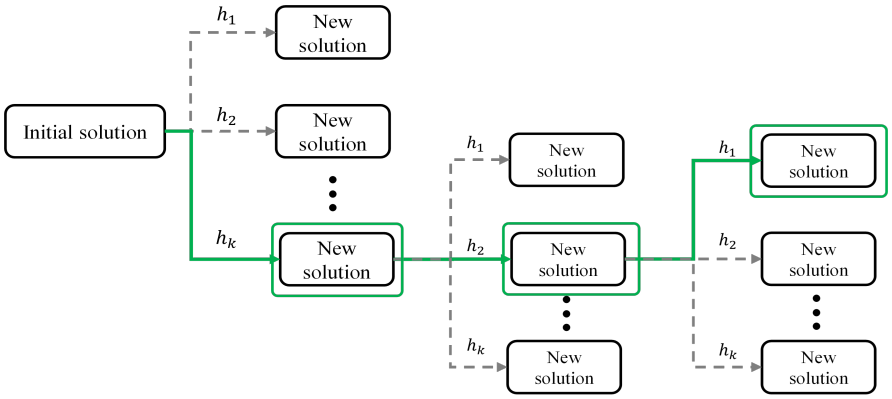

Figure 1: Flowchart of the multi-neighborhood search algorithm used in the search phase of the rGRASP.

Different construction heuristics can be used in GRASP, where many of these rely on a parameter α that restricts the candidate list to high-quality elements. While traditional approaches use a fixed value for α, the reactive approach used in the present work selects α from a predefined set of values using selection probabilities that are updated iteratively (Prais and Ribeiro, 2000). This adaptation reduces the need for manual tuning and improves robustness and solution quality (Resende and Ribeiro, 2016). Moreover, the parallelized version of this algorithm exploits the independence that exists between each GRASP iteration by running each in an independent thread. Communication between threads occurs by using a pool of elite solutions, enabling near-linear speed-ups and enhancing solution improvement (Ribeiro and Rosseti, 2007).

3 A case study at a gold mining complex

The proposed method is applied to a gold mining complex consisting of two open pits, the first divided into four areas (A1–A4) and the second into two areas (A5–A6), as shown in Figure 2. The material is extracted and transported by a shared fleet of trucks and shovels to five possible destinations (Figure 3): a stockpile connected to the milling and grinding circuit, directly to the milling and grinding circuit, a secondary processing stream (heap leach facility), or one of the two available waste dumps. As shown in Figure 3, Mine 1 can only send material to Waste Dump 1, while Mine 2 can only send material to Waste Dump 2, while all other locations are available for both mines. Given the operational capacities, the mill and grinding circuit are limited to a maximum throughput of 360,000 tons of ore and a minimum of 60,000 tons. Additionally, the available truck and shovel fleet imposes a monthly mining extraction limit of 700,000 tons.

The optimization focuses on short-term production scheduling over a one-year planning horizon, discretized into 12 periods (months). Mine 1 is composed of 4,754 blocks while Mine 2 is composed of 1,628 blocks, each of size $15 \times 15 \times 12\text{m}^3$.These blocks only represent the portion of the deposit selected from the long-term plan for extraction during the year. The main source of geological uncertainty arises from the variability in gold grades, which is modelled using 15 equally probable orebody scenarios generated using geostatistical simulation techniques (Goovaerts, 1997). The economic parameters and penalty costs used during the optimization are presented in Tables 4 and 5, respectively.

The truck fleet is divided into two truck types: small trucks with a capacity of 100 tons and large trucks with a capacity of 140 tons. Operational constraints impose a minimum of 5 and 7 trucks, and a maximum of 8 and 11 trucks, for the small and large truck types, respectively. Stochastic truck-availability scenarios are generated via Monte Carlo sampling from distributions retrieved from operational data. Operating costs are assumed to be 124 US dollars per hour for the small trucks and 176 US dollars per hour for the larger ones. Similar to Both and Dimitrakopoulos (2020), four shovels

are available in the complex with variable production rates (Table 6). Each time a shovel is reallocated between areas, movement costs and temporary production losses occur, as observed in Table 7.

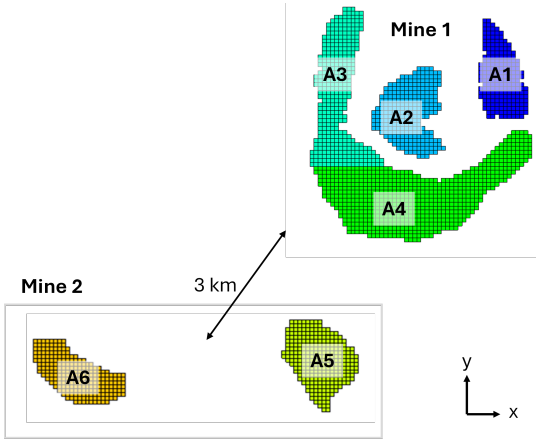

Figure 2: Layout of the gold mining complex showing individual mines and their division into areas.

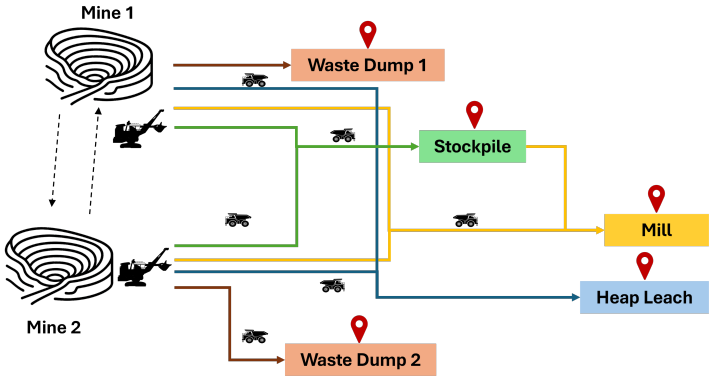

Figure 3: Schematic diagram of the gold mining complex used in the case study.

Table 4: Economic parameters from the mining complex.

Parameter	Value	Unit
Gold price	1250	US$/oz
Refinery cost	13	US$/oz
Leach cost	2.30	US$/t
Leach recovery	45	%
Mill cost	7.80	US$/t
Mill recovery	88	%
Stockpile rehandling cost	0.15	US$/t
Shovel operational costs	950	US$/h

Table 5: Penalties costs applied to each production target deviation considered in the optimization.

Production target	Penalty costs	Unit
Mining capacity	80.0	US$/ton
Mill capacity (Upper)	80.0	US$/ton
Mill capacity (Lower)	150.0	US$/ton
Shovel production	10.0	US$/ton
Truck fleet production	10.0	US$/ton
Smoothness	30,000.0	US$/block

Table 6: Expected production rates statistics from the shovels based on historical data.

Shovel equipment	Production rates (t/h) Mean	Production rates (t/h) Standard Deviation
Small Shovel 1	2597	129.8
Small Shovel 2	2538	126.9
Large Shovel 1	1310	65.5
Large Shovel 2	1283	64.1

Table 7: Relocation cost (kUS$) and associated production loss (ktons) for moving shovels between areas (A1–A6). Each cell indicates the cost and the tons of production lost when moving a shovel from the row area to the column area, respectively.

	To A1	To A2	To A3	To A4	To A5	To A6
From A1	0.0/0.0	2.9/15.6	4.3/23.4	3.4/18.2	19.5/106.6	10.0/98.8
From A2	3.3/18.2	0.0/0.0	5.2/28.6	5.3/28.6	20.0/109.2	18.5/101.4
From A3	4.8/26	4.3/23.4	0.0/0.0	1.9/10.4	20.0/109.2	18.5/101.4
From A4	3.8/20.8	4.8/26	1.4/7.8	0.0/0.0	19.5/106.6	18.5/101.4
From A5	20.4/111.8	20.4/111.8	21.9/119.6	20.0/109.2	0.0/0.0	4.3/23.4
From A6	19.0/104	19.5/106.6	20.4/111.8	18.5/101.4	3.8/20.8	0.0/0.0

3.1 Carbon footprint parameters

The fuel consumption parameters are assumed to be known in advance and account for the combined effects of distance, road slopes, and equipment characteristics. For trucks, $\widetilde{FCtruck}_{b,s,m}$ denotes the fuel (liters) required to transport a block b to a designated destination defined under geological scenario s using a truck-type m. This includes factors such as loaded gross vehicle weight (GVW), empty weight, and haul road conditions. For shovels, $FC_{l,a,a'}$ represent the fuel (liters) consumed when moving a shovel l from an area a to another area $a^{'}$, considering shovel characteristics and the slope and distance between areas. To compute the energy consumed, Equations (7) and (8) are used by the model. A fuel density factor (ρ) of 0.85 kilograms per liter with a diesel HHV (δ) of 45,500 kilojoules per kilogram of burned fuel is used to compute the total energy consumed from fuel combustion.

As presented in Section 2.1.3, α_{b,m,s_o} is modeled stochastically and discretized into the s_o scenarios. To ensure feasibility, the sum of proportions across all truck types ($\sum_{m\in\mathbb{M}} \alpha_{b,m,s_o}$) for a given block and operational scenario cannot exceed 1. For each block-truck type combination, values of α_{b,m,s_o} are conditionally sampled (given the proportions already assigned to other truck types) from a uniform distribution and adjusted so that the transported material divided by the truck capacity correspond to an integer number of trips for all truck types. In this study, the number of scenarios generated are limited to five to control computational complexity. Preliminary optimization trials showed that including more than five scenarios (leading to more than 6,750 joint scenarios once combined with geological, equipment, and carbon scenarios) exponentially increased solution times.

As shown in Equation (10), carbon footprint factors (CF_{s_c}) are required to compute the total expected carbon footprint indicator. These factors are calculated using default emission factors ($Ef^e_{s_c}$) for off-road mobile sources and machinery given by the 2006 IPCC Guidelines (IPCC, 2006). The emission factors quantify the mass of each gas emitted per unit of energy consumed and are defined as ranges between lower and upper bounds. As presented in Equation (9), these factors are multiplied by their respective characterization factor (f_e) from Fouli et al. (2021), converting emissions into carbon dioxide equivalents (CO_2-eq.) to reflect their global warming potential. The contribution of each emission to the carbon footprint indicator is summarized in Table 8.

Each scenario s_c is generated by combining one of the three representative values (lower, average, upper) for each of the three greenhouse gases considered, using Equation (9). This approach allows the model to explore the full range of plausible carbon footprint outcomes, while maintaining computational tractability. Preliminary optimization trials showed that, since emissions are bounded by these lower

Table 8: Emission factors used to estimate the carbon footprint indicator.

Emission	Lower value [kg CO_2-eq./TJ]	Average value [kg CO_2-eq./TJ]	Upper Value [kg CO_2-eq./TJ]
Carbon dioxide (CO2)	72,600	73,700	74,800
Methane (CH4)	46.76	168.98	291.2
Nitrous oxide (N2O)	4,261.4	14,914.9	25,568.4

and upper limits, considering a large number of scenarios adds no value to the assessment. Therefore, nine carbon footprint scenarios are considered in this study that reflect the combination of the three representative values for each of the three GHG emissions considered.

The optimization model uses carbon footprint limits (CF_t^{limit}) to compute deviations. An upper bound is established based on Canada's Output-based Carbon Pricing System (OBPS) regulations (SOR/2019-266). These regulations define carbon footprint limits according to the average annual metal production, an output-based standard of 7.71 tons of CO_2 eq. per kilogram of gold produced, the applicable calendar year, and other regulatory factors. For this study, a fixed upper limit of 652 tons of CO_2-eq. per month is adopted.

To evaluate the impact of incorporating the carbon footprint into the optimization, three cases were analyzed. 1) Baseline (BL) case: no carbon footprint charges were considered; 2) Just Over (JO) case: a penalty of 95$ per ton of CO_2-eq. emitted (reflecting Canada's federal benchmark price in 2025) was applied for exceeding the carbon footprint limit; 3) Full Incentive (FI) case: using the same penalty as the JO case plus a reward 50% higher than the penalty for staying below the limits to study the effects of a different carbon pricing scheme (stronger incentive to decarbonize).

3.2 Results and discussion

Figure 4a and Figure 4b present the risk profiles of the material extracted from the mines and the material sent to the mill, respectively, across all analyzed scenarios and periods. The figures show the results from the risk assessment, where the 10^{th} (P10), and 90^{th} (P90) percentiles for each period are presented with dashed lines, and the 50^{th} (P50) is presented with a solid line. It is worth noting that, in Figure 4a, no dashed lines appear, since there is no uncertainty in the tonnages extracted from the mines. The results show that, by introducing different carbon footprint pricing scenarios into the optimization, only minor variations are observed in the total amount of material extracted from the mines per month. This can be primarily attributed to how the model is constrained to extract all the material predefined by the long-term plan, which is implemented as a hard constraint in the mathematical formulation. In addition, the continuous requirement to supply sufficient material to the Mill, which is bounded by lower and upper processing limits (Figure 4b), further restricts the solution space.

Figure 5 shows the tisk profiles for each scenario of the cumulative material at each location. The cumulative material sent to the Mill exhibits notable differences between carbon pricing strategies, as can be observed from Figure 5a. The figure shows that the differences stem from including carbon pricing scenarios, which influence the destination policy. For instance, under the FI scenario, more material is allocated to the mill in later periods; however, the overall quantity directed to this location is lower (−16.1%), as shown in Figure 5a, a trend also observed under the JO scenario (−17.0%). Similarly, less material is sent to the leach pad in scenarios where carbon pricing systems are included (Figure 5b). These results emphasize the influence of the carbon pricing scenarios on destination policies. However, this result should not be overgeneralized, as different spatial configurations, such as varying distances between destinations, may lead to different results.

From the material received at the Waste Dump and the Stockpile, shown in Figure 5c and Figure 5d, respectively, it is evident that more material is consistently allocated to these lower-emission

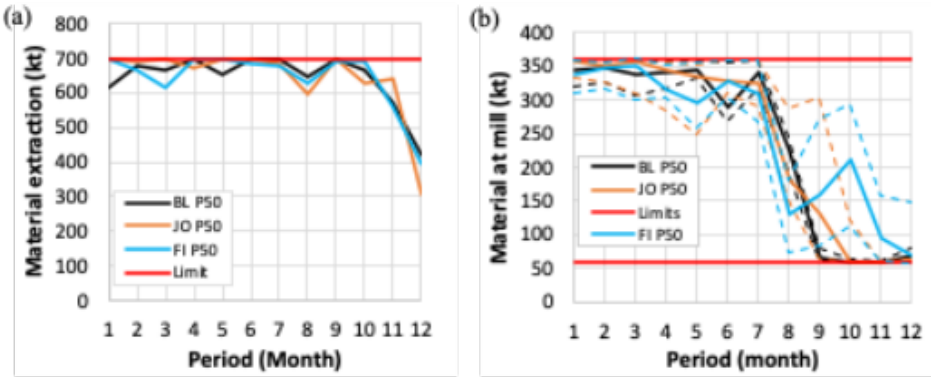

Figure 4: Risk profiles for each scenario of the material extracted from the mine (a) and the mill (b). Continuous lines represent the P50, while dotted lines represent the P10 and P90 values.

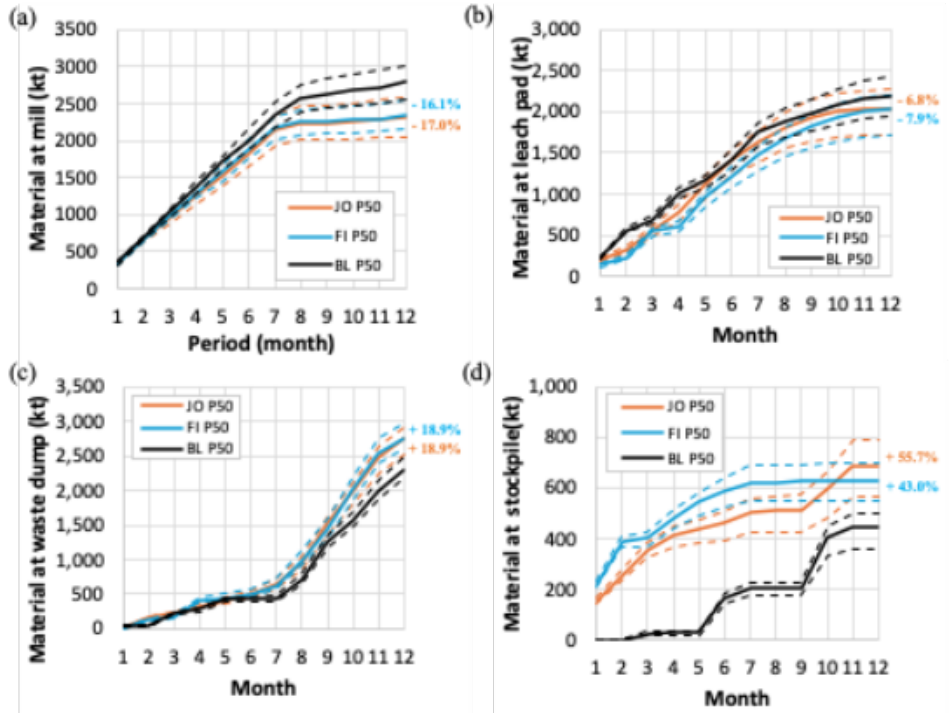

Figure 5: Risk profiles for each scenario of the cumulative material at each location. Continuous lines represent the P50, while dotted lines represent the P10 and P90 values.

destinations under stricter carbon pricing scenarios (JO and FI cases). Specifically, 18.9% more material is directed to the Waste Dump under both scenarios, while the Stockpile receives 55.7% and 43.0% more material under the JO and FI carbon pricing cases, respectively. This behavior suggests that marginal-grade material, which contributes little to economic value, is deprioritized and redirected to the nearest location in order to reduce carbon emissions.

From the P10 and P90 curves in Figure 5, it is clear that incorporating new sources of uncertainty into the optimization leads to a wider gap between the two percentiles. This result is expected, as the additional uncertainties are propagated through the entire mineral value chain and are amplified by the non-linear transfer functions used to model material flows and calculations. Similar widening behavior has also been reported in previous stochastic mine planning studies (Saliba and Dimitrakopoulos, 2019;

Jiang and Dimitrakopoulos, 2025), confirming that additional sources of uncertainty generally increase the spread of the risk profiles.

Figure 6 illustrates how the spatial assignment of each shovel changes across areas and scenarios for each month. Each row of the figure represents a shovel under a specific scenario, while each column represents a specific period (month). The interception of both led to the area (from area 1 to area 6) where each shovel is located. From the figure, it can be observed that shovel allocation tends to remain stable during the first and last four periods, whereas in intermediate periods the allocations deviate from the baseline across the different carbon scenarios. These deviations reflect the flexibility introduced in the scheduling process, allowing equipment deployment to be adjusted in order to reduce emissions while still meeting extraction requirements. This reallocation directly influences the total distance travelled by each shovel, as observed in Figure 7. This figure shows the distances travelled for each shovel under the different carbon footprint scenarios evaluated. For Shovel 1, the distance travelled in the baseline scenario is notably higher than in any of the carbon-pricing scenarios, indicating a more carbon-intensive routing under traditional conditions. However, for shovels 2, 3, and 4, the inclusion of carbon footprint constraints increases the total distance travelled. This counterintuitive outcome arises because travel distance is not minimized alone, but rather balanced along with multiple objectives, namely economic results, extraction sequence connectivity, deviation from production targets, and environmental impacts.

	Scenario \ Period	1	2	3	4	5	6	7	8	9	10	11	12
Shovel 1	*Baseline*	2	2	5	5	5	1	4	1	6	4	6	6
	Just Over	2	5	4	4	4	3	4	4	6	6	6	6
	Higher Under	2	1	4	5	4	4	5	4	6	6	6	6
Shovel 2	*Baseline*	1	4	4	3	4	4	4	3	3	4	6	4
	Just Over	2	5	4	4	4	5	5	4	3	3	4	4
	Higher Under	2	5	4	5	4	4	3	4	3	4	4	4
Shovel 3	*Baseline*	2	2	5	5	5	5	5	4	3	3	3	4
	Just Over	1	1	1	5	5	5	2	1	4	4	3	1
	Higher Under	1	2	1	1	3	3	4	3	4	3	3	3
Shovel 4	*Baseline*	1	4	4	4	4	4	2	2	1	3	3	2
	Just Over	1	1	2	2	2	4	1	3	3	3	3	3
	Higher Under	1	2	2	2	5	2	4	3	4	3	3	1

Figure 6: Locations of each shovel for each period and scenario.

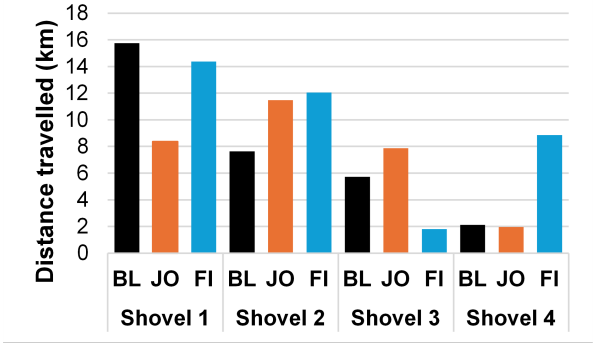

Figure 7: Comparison of total distance travelled for each shovel under each scenario.

Figure 8 shows a top view of the production schedule for each period (month) under each carbon footprint scenario. The figure shows that, as the sequencing shifts, so too does the spatial distribution of

active areas, prompting the reallocation of shovels in ways that may increase travel for some units while minimizing overall emissions. For example, it may be preferable to send a shovel with a lower emission rate (shovels 3 and 4) to a more distant high-tonnage area if it allows another shovel to serve a closer but less critical block, ultimately reducing the carbon footprint of the entire operation. Additionally, the figure depicts the solver's capabilities to generate contiguous extraction zones, where almost no stand-alone blocks can be observed. This behavior arises from the mathematical formulation, in which the smoothness component penalizes non-connectivity, thereby promoting smoother transitions and ensuring enough operational space for the equipment.

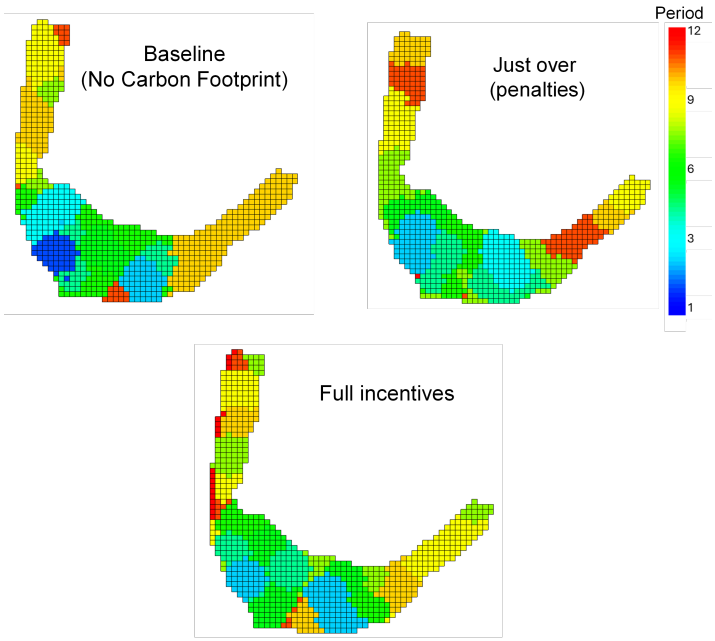

Figure 8: Top view comparing monthly extraction sequences across scenarios.

Figure 9 shows the 10^{th}, 50^{th}, and 90^{th} percentiles obtained from the risk assessment of the cumulative carbon footprint from shovel operations for each period. From the figure, it can be observed that emissions increase under the different carbon pricing scenarios. While this may appear counterintuitive, the outcome can be explained by the trade-offs between minimizing carbon emissions and achieving production efficiency during the optimization. As noted earlier with the distance travelled (Figure 7), multiple conflicting objectives are balanced, including material extraction targets, processing requirements, equipment constraints, and carbon footprint minimization.

In this context, the emissions generated by shovel movements represent a relatively small fraction of the total carbon footprint (Figure 9). As a result, decisions that have a larger impact on the overall emissions are prioritized, such as destination policies and extraction sequence, while accepting a modest increase in shovel-related emissions when it supports more efficient or lower-emission flows elsewhere in the system. This reflects the model's global perspective, where localized increases in one emission source may be justified if they enable greater reductions elsewhere.

Figure 10 presents the total carbon footprint obtained for each month under the three different scenarios evaluated. When analyzing the risk profile of the carbon footprint on a month-by-month basis (Figure 10a), it becomes evident that the incorporation of carbon pricing has only a marginal impact on monthly emission levels. This limited effect suggests that the current carbon pricing strategies are not strong enough to significantly influence short-term operational decisions. However, when looking at the cumulative impact over the entire planning horizon (Figure 10b), resulting from the changes in the material destination policy, even though the month-to-month impact may appear minimal, these

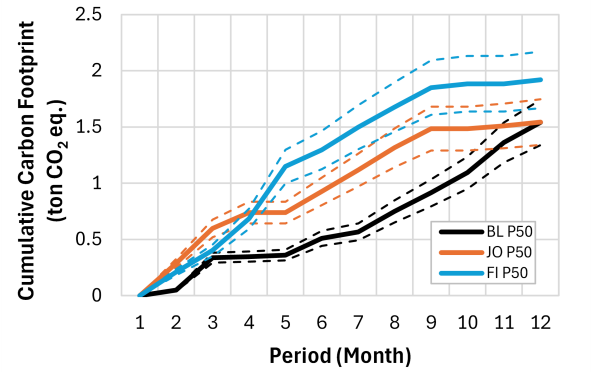

Figure 9: Cumulative carbon footprint obtained from the shovel movement.

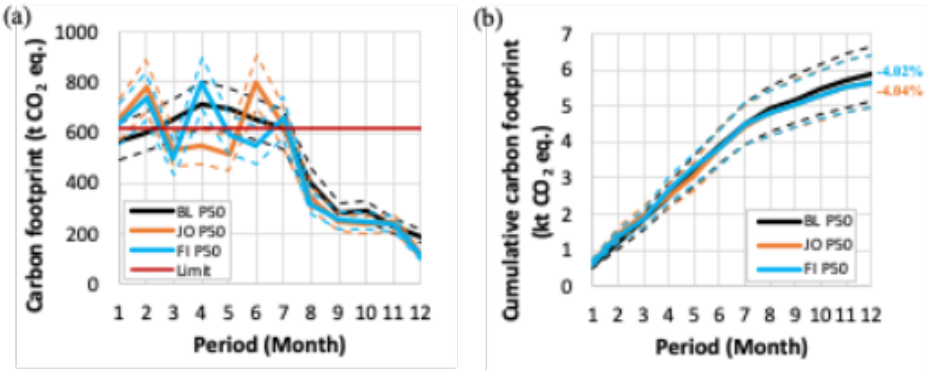

Figure 10: Carbon footprint and cumulative carbon footprint risk profiles per month.

small adjustments accumulate over time and result in an overall reduction of 4.0% in the total carbon footprint indicator.

As a result of incorporating both bonuses and penalties as a strategy to reduce environmental impacts, the overall carbon footprint is reduced while maintaining economic viability. Figure 11 presents the cumulative profit per period (month) obtained for each of the scenarios evaluated. Specifically, the figure shows that when an FI strategy is applied, the total profit decreases by only 0.4% ($-\$233,839$), whereas a JO approach leads to a slightly larger reduction of 1.0% ($-\$611,890$). In other words, with the FI strategy, each 1% reduction in the carbon footprint indicator corresponds to a 0.1% decrease in profit, while under the JO strategy, each 1% reduction results in a 0.25% decrease in profit. These results demonstrate that low economic trade-offs can yield meaningful environmental benefits; this is in contrast with prior studies, which found that, for each 1% reduction in the environmental indicator, there is more than a 0.5% decrease in profit (Xu et al., 2018; Pell et al., 2019; Xu et al., 2021). Moreover, previous studies have focused on long-term mine production planning, where more flexibility exists because blocks can be excluded from the extraction, if necessary. By contrast, the short-term context considered here involves strict production scheduling, where all the material must be extracted and allocated. This highlights the capabilities of the proposed approach in managing trade-offs and uncertainty under more constrained and operationally realistic conditions.

Another important finding is that, in the FI scenario, most of the economic value is obtained toward the end of the year. This outcome stems from the spatial variability of the gold grades, where higher grades become available later in the year and are scheduled accordingly to manage the uncertainties associated with carbon emissions.

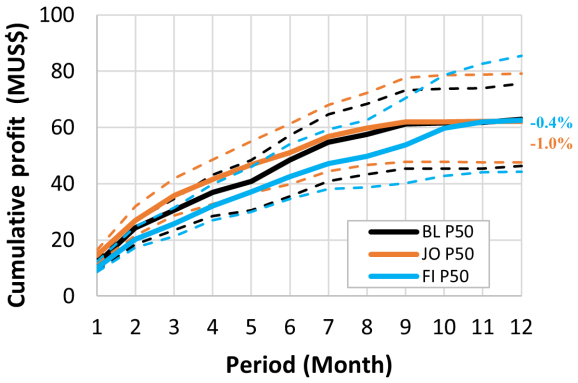

Figure 11: Cumulative profit per month obtained for each carbon footprint pricing scenario.

4 Conclusions and future work

This study introduces a novel optimization framework that integrates carbon footprint considerations directly into the joint decision-making process of material extraction scheduling and fleet management. By evaluating different carbon pricing scenarios, the results demonstrate that meaningful reductions in emissions can be achieved with minimal impact on economic performance. Specifically, simultaneous optimization under uncertainty enables the model to capture the trade-offs between operational efficiency and environmental impact. The proposed approach achieves a 4% reduction in the overall carbon footprint while incurring only a 0.4% decrease in total profit under a full incentive scenario. This reduction can be seen as a marginal trade-off for complex and real-world scenarios, given the relatively short computational times achieved. Moreover, past studies have shown that similar reductions in environmental impacts were often necessarily accompanied by significantly larger profit losses, which highlights the efficiency and practical relevance of the proposed approach.

The integration of carbon pricing mechanisms, whether through penalties, incentives, or both, guides the system toward more sustainable decisions, particularly changing the destination policies, equipment allocation, and extraction schedule. Despite minor reductions in profit, the results confirm that decarbonization objectives can be pursued alongside production targets in a balanced and cost-effective manner under uncertain scenarios.

Additionally, a new solution approach is introduced and adapted to address the simultaneous stochastic optimization of mining complexes. The reactive Greedy Randomized Adaptive Search Procedure with cooperative parallelization proves to be effective in solving this complex, non-linear problem, supporting future applications in stochastic mine production planning.

Future work should incorporate new sources of carbon emissions, such as energy consumption in downstream processes, which are known to be significant contributors to the overall environmental impact of mining operations. In particular, emissions associated with crushing, grinding, and other comminution stages are among the most energy-intensive activities in mineral processing (Ballantyne and Powell, 2014; Jeswiet and Szekeres, 2016). Considering the sensitivity of processing plant efficiency to the geometallurgical characteristics of the material, their inclusion, along with their related uncertainty in the optimization process, should also be worth exploring. This would allow the model to capture how the variability in geometallurgical properties influence energy use, throughput, efficiency, and recovery rates, thereby refining both the operational plan and its associated carbon footprint (Dimitrakopoulos and Lamghari, 2022). Incorporating such downstream dynamics can, ultimately, lead to more accurate predictions of energy consumption and more effective strategies for reducing emissions across the entire mineral value chain, capitalizing on the synergies that arise from a mine-to-mill approach under uncertain scenarios.

Future research should also extend the proposed solver to long-term mine planning by adapting its construction phase and leveraging its scalability for larger, more complex models. Finally, further work should also explore alternative search algorithms and the integration of robust machine learning-based solvers (Yaakoubi and Dimitrakopoulos, 2023; 2025) and decision trees with deep reinforcement learning (Kumar and Dimitrakopoulos, 2021), which have shown potential to improve both solution quality and computational efficiency within the GRASP framework.

References

Aiex, R. M., Resende, M. G., and Ribeiro, C. C. (2002). Probability distribution of solution time in grasp: an experimental investigation. Journal of Heuristics, 8, 343–373. https://doi.org/10.1023/A:1015061802659

Amegboleza, A. A., and Ülkü, M. A. (2025). Sustainable energy transition for the mining industry: a bibliometric analysis of trends and emerging research pathways. Sustainability, 17(5), 2292. https://doi.org/10.3390/su17052292

Amirmoeini, B., Grenon, M., and Moradi Afrapoli, A. (2024). Towards sustainable mining: GHG considerate open pit long-term planning using adaptive large neighborhood search algorithm In Mining Optimization Laboratory (MOL) – Report Twelve, 2023/2024 (pp. 244–262). University of Alberta. https://sites.ualberta.ca/MOL/DataFiles/2024_Papers/301_Amirmoeini.pdf

Ballantyne, G. R., and Powell, M.S. (2014). Benchmarking comminution energy consumption for the processing of copper and gold ores. Minerals Engineering, 65, 109-114. https://doi.org/10.1016/j.mineng.2014.05.017

Birge, J. R., and Louveaux, F. (2011). Introduction to stochastic programming (2nd ed.). Springer. https://doi.org/10.1007/978-1-4614-0237-4

Blom, M., Pearce, A. R., and Stuckey, P. J. (2017). Short-term scheduling of an open-pit mine with multiple objectives. Engineering Optimization, 49(5), 777–795. https://doi.org/10.1080/0305215X.2016.1218002

Both, C., and Dimitrakopoulos, R. (2020). Joint stochastic short-term production scheduling and fleet management optimization for mining complexes. Optimization and Engineering, 21(4), 1717–1743. https://doi.org/10.1007/s11081-020-09495-x

Calderon, J. L., Bazilian, M., Sovacool, B., Hund, K., Jowitt, S. M., Nguyen, T. P., Månberger, A., Kah, M., Greene, S., Galeazzi, C., Awuah-Offei, K., Moats, M., Tilton, J., and Kukoda, S. (2020). Reviewing the material and metal security of low-carbon energy transitions. Renewable and Sustainable Energy Reviews, 124, 109789. https://doi.org/10.1016/j.rser.2020.109789

Carvalho, F. P. (2017). Mining industry and sustainable development: Time for change. Food and Energy Security, 6(2), 61–77. https://doi.org/10.1002/fes3.109

De Donno, M. G. (2024). Metals for the energy transition: Exploring opportunities amidst supply-demand imbalance. In SPE Europec featured at EAGE Conference and Exhibition. Society of Petroleum Engineers. https://doi.org/10.2118/219988-MS

Dimitrakopoulos, R., and Ramazan, S. (2004). Uncertainty based production scheduling in open pit mining. SME Transactions, 316, 106–112.

Dimitrakopoulos, R., and Lamghari, A. (2022). Simultaneous stochastic optimization of mining complexes - mineral value chains: an overview of concepts, examples and comparisons. International Journal of Mining, Reclamation and Environment, 36(6), 443–460. https://doi.org/10.1080/17480930.2022.2065730

Eggleston, H. S., Buendia, L., Miwa, K., Ngara, T., and Tanabe, K. (2006). 2006 IPCC guidelines for national greenhouse gas inventories: Volume 2: Energy – Chapter 3: Mobile combustion. Intergovernmental Panel on Climate Change (IPCC). https://www.ipcc-nggip.iges.or.jp/public/2006gl/pdf/2_Volume2/V2_3_Ch3_Mobile_Combustion.pdf

Festa, P., and Resende, M. G. C. (2002). GRASP: An annotated bibliography. In S. Voss, S. Martello, I. Osman, and C. Roucairol (Eds.), Essays and surveys in metaheuristics (pp. 325–367). Springer. https://doi.org/10.1007/978-1-4615-1507-4_15

Fioroni, M., Franzese, L. A., Bianchi, T., Ezawa, L., Pinto, L., and de Miranda Jr., G. (2008). Concurrent simulation and optimization models for mine planning. In S. J. Mason, R. R. Hill, L. Mönch, O. Rose, T. Jefferson, and J. W. Fowler (Eds.), Proceedings of the 2008 Winter Simulation Conference (pp. 759–767). Winter Simulation Conference.

Fouli, Y., Hurlbert, M., and Kröbel, R. (2021). Greenhouse gas emissions from Canadian agriculture: Estimates and measurements. The School of Public Policy Publications, 14(1). https://doi.org/10.11575/sppp.v14i1.72445

Goodfellow, R. C., and Dimitrakopoulos, R. (2016). Global optimization of open pit mining complexes with uncertainty. Applied Soft Computing, 40, 292–304. https://doi.org/10.1016/j.asoc.2015.11.038

Goodfellow, R., and Dimitrakopoulos, R. (2017). Simultaneous stochastic optimization of mining complexes and mineral value chains. Mathematical Geosciences, 49, 341–360. https://doi.org/10.1007/s11004-017-9680-3

Goovaerts, P. (1997). Geostatistics for natural resources evaluation. Oxford university press.

Huo, D., Sari, Y. A., Kealey, R., and Zhang, Q. (2023). Reinforcement learning-based fleet dispatching for greenhouse gas emission reduction in open-pit mining operations. Resources, Conservation and Recycling, 188, 106664. https://doi.org/10.1016/j.resconrec.2022.106664

Jeswiet, J., and Szekeres, A. (2016). Energy consumption in mining comminution. Procedia CIRP, 48, 140-145.

Jiang, Y., and Dimitrakopoulos, R. (2024). An application of simultaneous stochastic optimisation on an open-pit copper mining complex with supply, recovery, and market uncertainties. International Journal of Mining, Reclamation and Environment, 39(1), 74–92. https://doi.org/10.1080/17480930.2024.2381904

Kamran, M., Raugei, M., and Hutchinson, A. (2023). Critical elements for a successful energy transition: A systematic review. Renewable and Sustainable Energy Transition, 4, 100068. https://doi.org/10.1016/j.rset.2023.100068

Kozan, E., and Liu, S. Q. (2018). An open-pit multi-stage mine production scheduling model for drilling, blasting and excavating operations. In R. Dimitrakopoulos (Ed.), Advances in applied strategic mine planning (pp. 655–668). Springer. https://doi.org/10.1007/978-3-319-69320-0_39

Kumar, A., and Dimitrakopoulos, R. (2021). Production scheduling in industrial mining complexes with incoming new information using tree search and deep reinforcement learning. Applied Soft Computing, 110, 107644. https://doi.org/10.1016/j.asoc.2021.107644

Lamghari, A. and Dimitrakopoulos, R. (2012). A diversified Tabu search approach for the open-pit mine production scheduling problem with metal uncertainty. European Journal of Operational Research, 222(3), 642–652. https://doi.org/10.1016/j.ejor.2012.05.029

Lamghari, A., Dimitrakopoulos, R., and Ferland, J. A. (2014). A variable neighbourhood descent algorithm for the open-pit mine production scheduling problem with metal uncertainty. Journal of the Operational Research Society, 65(9), 1305–1314. https://doi.org/10.1057/jors.2013.81

Lamghari, A. and Dimitrakopoulos, R. (2020). Hyper-heuristic approaches for strategic mine planning under uncertainty. Computers and Operations Research, 115, 104590. https://doi.org/10.1016/j.cor.2018.11.010

Lamghari, A. and Dimitrakopoulos, R. (2022). An adaptive large neighborhood search heuristic to optimize mineral value chains under metal and material type uncertainty. International Journal of Mining, Reclamation and Environment, 36(1). https://doi.org/10.1080/17480930.2021.1949858

Laurence, D. (2011). Establishing a sustainable mining operation: An overview. Journal of Cleaner Production, 19(2–3), 278–284. https://doi.org/10.1016/j.jclepro.2010.08.019

Liu, L., Ji, H., Lü, X., Zhang, J., and Lu, J. (2021). Mitigation of greenhouse gases released from mining activities: A review. International Journal of Minerals, Metallurgy and Materials, 28, 513–521. https://doi.org/10.1007/s12613-020-2155-4

L'Heureux, G., Gamache, M., and Soumis, F. (2013). Mixed integer programming model for short-term planning in open-pit mines. Mining Technology, 122(2), 101–109. https://doi.org/10.1179/1743286313Y.0000000037

Matthews, H. S., Hendrickson, C. T., and Weber, C. L. (2008). The importance of carbon footprint estimation boundaries. Environmental Science and Technology, 42(16), 5839–5842. https://doi.org/10.1021/es703112w

Miranda, C. E., and Pourrahimian, Y. (2024). Technological advances in mobile equipment for greenhouse gas emission reduction in the mining industry: A systematic review. In Mining Optimization Laboratory (MOL) – Report Twelve, 2023/2024 (pp. 263–275). University of Alberta. https://sites.ualberta.ca/MOL/DataFiles/2024_Papers/302_Miranda.pdf

Mirzehi, M., and Moradi Afrapoli, A. (2024a). Dust and greenhouse gas mitigation in mining: An LCA-MILP approach to sustainable open-pit planning. In Mining Optimization Laboratory (MOL) – Report Twelve, 2023/2024 (pp. 276–293). University of Alberta. https://sites.ualberta.ca/MOL/DataFiles/2024_Papers/303_Mirzehi.pdf

Mirzehi, M., and Moradi Afrapoli, A. (2024b). Sustainable mine planning: An integrated framework for balancing economic and environmental costs in open-pit mining. In Mining Optimization Laboratory (MOL) – Report Twelve, 2023/2024 (pp. 294–313). University of Alberta.

Mirzehi, M., and Moradi Afrapoli, A. (2024c). Balancing economic viability and environmental stewardship in open-pit mining: A multi-objective optimization approach. In Mining Optimization Laboratory (MOL) – Report Twelve, 2023/2024 (pp. 314–328). University of Alberta. https://sites.ualberta.ca/MOL/DataFiles/2024_Papers/305_Mirzehi.pdf

Montiel, L., and Dimitrakopoulos, R. (2015). Optimizing mining complexes with multiple processing and transportation alternatives: An uncertainty-based approach. European Journal of Operational Research, 247(1), 166–178. https://doi.org/10.1016/j.ejor.2015.05.002

Montiel, L., Dimitrakopoulos, R. (2017). A heuristic approach for the stochastic optimization of mine production schedules. Journal of Heuristics, 23, 397–415. https://doi.org/10.1007/s10732-017-9349-6

Mora, C., Spirandelli, D., Franklin, E. C., Lynham, J., Kantar, M. B., Miles, W., Smith, C.Z., Freel, K., Moy, J., Louis, L.V., Barba, E.W., Bettinger, K., Frazier, A.G., Colburn IX, J.F., Hanasaki, N., Hawkins, E., Hirabayashi, Y., Knorr, W., Little, C.M., Emanuel, K., Sheffield, J., Patz, J.A., and Hunter, C. L. (2018). Broad threat to humanity from cumulative climate hazards intensified by greenhouse gas emissions. Nature Climate Change, 8(12), 1062–1071. https://doi.org/10.1038/s41558-018-0315-6

Moran, C. J., Lodhia, S., Kunz, N. C., and Huisingh, D. (2014). Sustainability in mining, minerals and energy: New processes, pathways and human interactions for a cautiously optimistic future. Journal of Cleaner Production, 84, 1–15. https://doi.org/10.1016/j.jclepro.2014.09.016

Mousavi, A., Kozan, E., and Liu, S. Q. (2016). Open-pit block sequencing optimization: A mathematical model and solution technique. Engineering Optimization, 48(11), 1932–1950. https://doi.org/10.1080/0305215X.2016.1142080

Nema, P., Nema, S., and Roy, P. (2012). An overview of global climate changing in current scenario and mitigation action. Renewable and Sustainable Energy Reviews, 16(4), 2329–2336. https://doi.org/10.1016/j.rser.2012.01.044

Nikbin, R., Bagherpour, R., Purhamadani, E., and Taherinia, A. (2025). Enhancing sustainability in mining by reducing hauling energy consumption through optimization of distance and slope with semi-mobile in-pit crushers and conveyors. Scientific Reports, 15(1), 22119. https://doi.org/10.1038/s41598-025-06534-4

Norgate, T., and Haque, N. (2010). Energy and greenhouse gas impacts of mining and mineral processing operations. Journal of Cleaner Production, 18(3), 266–274. https://doi.org/10.1016/j.jclepro.2009.09.020

Pell, R., Tijsseling, L., Palmer, L. W., Glass, H. J., Yan, X., Wall, F., Zeng, X., and Li, J. (2019). Environmental optimisation of mine scheduling through life cycle assessment integration. Resources, Conservation and Recycling, 142, 267–276. https://doi.org/10.1016/j.resconrec.2018.11.022

Prais, M., and Ribeiro, C. C. (2000). Reactive GRASP: An application to a matrix decomposition problem in TDMA traffic assignment. INFORMS Journal on Computing, 12(3), 164–176. https://doi.org/10.1287/ijoc.12.3.164.12639

Quigley, M., and Dimitrakopoulos, R. (2020). Incorporating geological and equipment performance uncertainty while optimising short-term mine production schedules. International Journal of Mining, Reclamation and Environment, 34(5), 362–383. https://doi.org/10.1080/17480930.2019.1658923

Rachid, S., Yassine, T. A. H. A., and Benzaazoua, M. (2023). Environmental evaluation of metals and minerals production based on a life cycle assessment approach: A systematic review. Minerals Engineering, 198, 108076. https://doi.org/10.1016/j.mineng.2023.108076

Resende, M. G. C., and Ribeiro, C. C. (2016). Extended construction heuristics. In Optimization by GRASP (pp. 119–134). Springer. https://doi.org/10.1007/978-1-4939-6530-4_7

Ribeiro, C. C., and Rosseti, I. (2007). Efficient parallel cooperative implementations of GRASP heuristics. Parallel Computing, 33(1), 21–35. https://doi.org/10.1016/j.parco.2006.11.007

Saliba, Z., and Dimitrakopoulos, R. (2019). Simultaneous stochastic optimization of an open pit gold mining complex with supply and market uncertainty. Mining Technology, 128(4), 216–229. https://doi.org/10.1080/25726668.2019.1626169

Suorineni, F. T. (2022). Challenges and implications for the mining industry for future resources extraction. International Journal of the Society of Materials Engineering for Resources, 25(1), 10–17. https://doi.org/10.5188/ijsmer.25.10

Torkamani, E., and Askari-Nasab, H. (2015). A linkage of truck-and-shovel operations to short-term mine plans using discrete-event simulation. International Journal of Mining and Mineral Engineering, 6(2), 97–111. https://doi.org/10.1504/IJMME.2015.070367

Vallée, M. (2000). Mineral resource + engineering, economic and legal feasibility = ore reserve. CIM Bulletin, 93(1038), 53–61.

Villalba Matamoros, M. E., and Dimitrakopoulos, R. (2016). Stochastic short-term mine production schedule accounting for fleet allocation, operational considerations and blending restrictions. European Journal of Operational Research, 255(3), 911–921. https://doi.org/10.1016/j.ejor.2016.05.050

Wiedmann, T., and Minx, J. (2008). A definition of 'carbon footprint'. Ecological Economics Research Trends, 1, 1–11.

Xu, X. C., Gu, X. W., Wang, Q., Gao, X. W., Liu, J. P., Wang, Z. K., and Wang, X. H. (2018). Production scheduling optimization considering ecological costs for open pit metal mines. Journal of Cleaner Production, 180, 210–221. https://doi.org/10.1016/j.jclepro.2018.01.135

Xu, X. C., Gu, X. W., Wang, Q., Zhao, Y. Q., and Wang, Z. K. (2021). Open pit limit optimization considering economic profit, ecological costs and social benefits. Transactions of Nonferrous Metals Society of China, 31(12), 3847–3861. https://doi.org/10.1016/S1003-6326(21)65769-2

Yaakoubi, Y., and Dimitrakopoulos, R. (2023). Learning to schedule heuristics for the simultaneous stochastic optimization of mining complexes. Computers and Operations Research, 159, 106349. https://doi.org/10.1016/j.cor.2023.106349

Yaakoubi, Y., and Dimitrakopoulos, R. (2025). Decision-focused neural adaptive search and diving for optimizing mining complexes. European Journal of Operational Research, 320(3), 699–719. https://doi.org/10.1016/j.ejor.2024.07.024

Yokoi, R., Watari, T., and Motoshita, M. (2022). Future greenhouse gas emissions from metal production: Gaps and opportunities towards climate goals. Energy and Environmental Science, 15(1), 146–157. https://doi.org/10.1039/D1EE02165F